Biocompatible, accurate, and fully autonomous: a sperm-driven micro-bio-robot

Islam S. M. Khalil, Veronika Magdanz, Samuel Sanchez, Oliver G. Schmidt & Sarthak Misra

Journal of Micro-Bio Robotics

ISSN 2194-6418
Volume 9
Combined 3-4

J Micro-Bio Robot (2014) 9:79-86
DOI 10.1007/s12213-014-0077-9

Springer

J Micro-Bio Robot (2014) 9:79–86
DOI 10.1007/s12213-014-0077-9

RESEARCH PAPER

Biocompatible, accurate, and fully autonomous: a sperm-driven micro-bio-robot

Islam S. M. Khalil · Veronika Magdanz · Samuel Sanchez · Oliver G. Schmidt · Sarthak Misra

Received: 6 March 2014 / Revised: 22 May 2014 / Accepted: 23 May 2014 / Published online: 13 June 2014

Abstract We study the magnetic-based motion control of a sperm-flagella driven Micro-Bio-Robot (MBR), and demonstrate precise point-to-point closed-loop motion control under the influence of the controlled magnetic field lines. This MBR consists of a bovine spermatozoon that is captured inside Ti/Fe nanomembranes. The nanomembranes are rolled-up into a 50 μm long microtube with a diameter of 5-8 μm. Our MBR is self-propelled by the sperm cell and guided using the magnetic torque exerted on the magnetic dipole of its rolled-up microtube. The self-propulsion force provided by the sperm cell allows the MBR to move at an average velocity of 25$\pm$10 μm/s towards a reference position, whereas the magnetic dipole moment and the controlled weak magnetic fields (approximately 1.39 mT) allow for the localization of the MBR within the vicinity of reference positions with an average region-of-convergence of 90$\pm$40μm. In addition, we experimentally demonstrate the guided motion of the MBR towards a magnetic microparticle with applications towards targeted drug delivery and microactuation.

Keywords Micro-bio-robot · Magnetic guidance · Sperm cells · Closed-loop · Motion control · Self-propulsion

Islam S. M. Khalil and Veronika Magdanz equally contributed towards the preparation of this work.

Electronic supplementary material The online version of this article (doi: 10.1007/s12213-014-0077-9) contains supplementary material, which is available to authorized users.

I. S. M. Khalil (✉)
German University in Cairo, New Cairo City 13411, Egypt
e-mail: islam.shoukry@guc.edu.eg

V. Magdanz · O. G. Schmidt
Institute for Integrative Nanosciences, IFW Dresden, Helmholtzstrasse 20, 01069 Dresden, Germany

V. Magdanz
e-mail: v.magdanz@ifw-dresden.de

O. G. Schmidt
Material Systems for Nanoelectronics, University of Technology Chemnitz, Chemnitz, Germany
e-mail: o.schmidt@ifw-dresden.de

S. Sanchez
Max Planck Institute for Intelligent Systems, Heisenbergstrasse 3, 70569 Stuttgart, Germany
e-mail: Sanchez@is.mpg.de

S. Misra
MIRA–Institute for Biomedical Technology and Technical Medicine, University of Twente, Enschede 7500AE, Netherlands
e-mail: s.misra@utwente.nl

1 Introduction

The design and locomotion of microrobotic systems have been inspired by nature to provide self-propulsion at low Reynolds numbers regimes [1]. These locomotion designs can be based on different propulsion mechanisms, including chemical [2], electrical [3], thermal and magnetic propulsion [4, 5], among others. Magnetic microrobots can be actuated by using oscillating [6] or rotating magnetic fields [4, 7]. Dreyfus et al. [6] and Bell et al. [8] have presented approaches to form flexible flagella using a one-dimensional flexible tail and a rigid helical tail, respectively. The former approach mimics the sperm-flagella to provide propulsion using external oscillating magnetic fields, while the latter is inspired by the *E. coli* bacteria and provides propulsion using external rotating magnetic fields. Nelson and Fischer reported the propulsion of small helical rigid microswimmers in rotating magnetic fields, and recent progress has been demonstrated in fabrication methods of that particular kind of structures [4, 9, 10]. One of the main challenges for the previously mentioned techniques is the fabrication at the microscale [5]. This challenge has motivated a few researchers to provide propulsion using living microorganisms such as magnetotactic bacteria and sperm cells [11–13].

Pan et al. have demonstrated the incorporation of magnetic nanoparticles inside live cells for direct protein sorting [14]. This incorporation allows for the magnetic control of live cells using external magnetic fields. However, the magnetic nanoparticles can affect vital functions of the cell due to their limited biocompatibility [15] if they pass through the cell membrane. This biocompatibility challenge can be overcome by combining motile cells with magnetic microobjects that are too large to be taken up by the cell. Magdanz et al. [11] have developed a Micro-Bio-Robot (MBR) by combining a motile sperm cell with a ferromagnetic rolled-up microtube [16, 17]. These tubes were manufactured with a diameter slightly larger than the sperm head to allow for mechanical coupling of the motile cell (Fig. 1). The coupling of the rolled-up microtube and the motile cell happens when a cell swims into one opening of the microtube. It becomes mechanically locked inside the tubular structure and starts pushing the microtube forward by the force of its flagellum. In this way the tail of the sperm provides the propulsion of the MBR and the thin ferromagnetic layer allows for the remote magnetic-based control (Fig. 2). Because of the synergistic properties mentioned above, the tubular system combined with biological propulsion can project important advances in the field of Micro-Bio-Robotics. The MBR reported by Magdanz and co-workers were rotated by a small permanent magnet positioned outside the system. This manual control mechanism is very imprecise and does not deliver reproducible motion control. Furthermore, the minimum required magnetic field strength with permanent magnets was estimated as 20 mT, which is much higher than what we measured with the system consisting of electromagnetic coils (Fig. 2).

In this study, we present advances in the remote control of the MBR, implementing a point-to-point closed-loop control, using four electromagnetic coils and feedback provided by a microscopic camera system. Implementation of point-to-point closed-loop control of the MBR is essential for the realization of future biomedical applications such as magnetically assisted fertilization [11], minimally invasive procedures [18], targeted drug delivery [19], cell manipulation and characterization [7], drilling of tissues [20, 21], and fixing cancer cells [10, 22]. This work demonstrates the point-to-point closed-loop motion control of MBRs under the influence of controlled magnetic fields in two-dimensional space using a previously developed electromagnetic system and control architecture [24, 25]. This magnetic control is accomplished by orienting the magnetic field lines towards a reference position. The feedback provided through a microscopic system allows the control system to direct the magnetic field lines towards the reference position to localize the MBR within its vicinity.

The remainder of this paper is organized as follows: Section 2 provides information about materials and methods of the fabrication of the microtubes and creation of the sperm-driven MBRs. Section 3 provides a brief description of the magnetic-based closed-loop control system that has been previously developed, and experimental closed-loop motion control results of the MBRs. Section 4 includes a discussion pertaining to possibilities of decreasing the size of the MBRs to make them viable for diverse biomedical applications. Finally, Section 5 concludes and provides directions for future work.

2 Materials and methods

The MBRs are developed by the fabrication of microtubes and coupling these tubes with sperm cells.

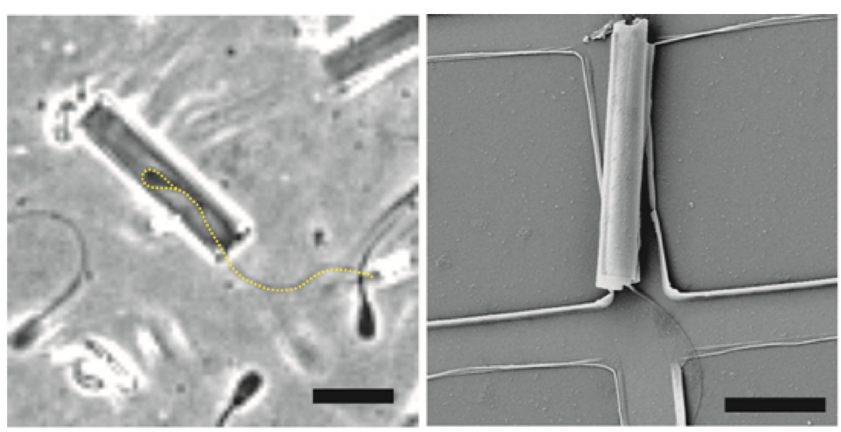

Fig. 1 Sperm-driven Micro-Bio-Robot consisting of a Ti/Fe microtube with length of 50 μm and a bovine sperm cell. *Left* Microscopic image of a microtube with a sperm cell. The *yellow dots* outline the bull spermatozoon. *Right* Scattering Electron Microscopy image of a microtube with a sperm cell (flagellum sticking out bottom of tube). *Scale bars* 20 μm

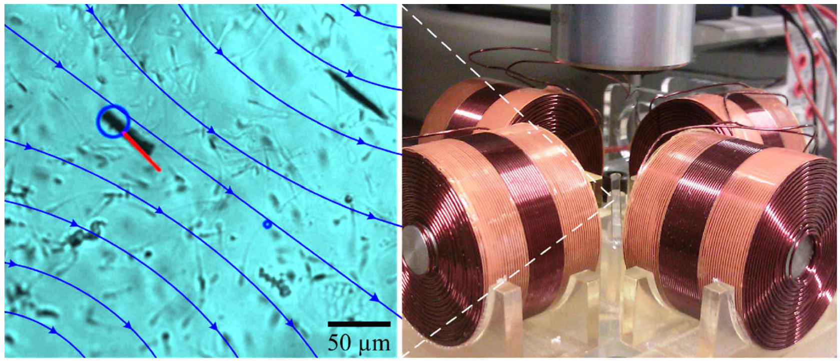

Fig. 2 An electromagnetic system [23, 25] for the wireless control of the Micro-Bio-Robot (MBR). The system consists of an orthogonal array of electromagnetic coils. Sperm cells and rolled-up microtube are contained inside a $1\times1\times1$ cm^3 glass vessel containing 1 mL cell solution. The inset shows a controlled MBR swimming towards a reference position (*blue circle*) under the influence of the controlled magnetic fields (*blue lines*) and the self-propulsion force

2.1 Fabrication of ferromagnetic microtubes by rolling up nanomembranes

The Ti/Fe microtubes are fabricated by rolling up thin layers using the method described in Mei et al. [16]. A 22×22 mm^2 glass substrate is coated with photoresist AR-P 3510, exposed to ultraviolet light for 7 seconds and developed with an AR 300-35: water (1:1) solution. A 12 nm thick layer of each, titanium and iron, are deposited onto the glass substrate using electron beam evaporation at a sample with angle of 75°. Strain engineering was used to design the rolled-up microtubes consisting of titanium and iron layers. The 75° angled deposition creates a "window" on the array. No material is deposited on one side of the photoresist squares due to the angled position of the sample. This window serves as starting point for the roll-up of the nanomembranes because the solvent etches the photoresist from this side first. The stress is implemented by a difference in deposition rate between the titanium (3 A/s) and iron (0.5-1 A/s) layers which cause the rolling of the nanomembranes upon release from the photoresist. The substrate is immersed in acetone which dissolves the photoresist layer. This process allows the Ti/Fe nanomembranes to roll-up immediately. Microtubes are formed with a length of 50 μm and a diameter of 5-10 μm. These microtubes are removed from the glass substrate by rinsing with a pipette or scratching the tube array with tweezers to release the microtubes. We chose titanium and iron for the fabrication of rolled-up microtubes, because titanium serves as a biocompatible adhesion layer between the photoresist and iron, and also induces a strain that is necessary for the roll-up. Iron was deposited as the ferromagnetic material inside the tubes.

We can adjust the fabrication parameters based on the desired materials, nanofilm thickness and template size during the fabrication process such that the resulting microtubes have a certain diameter, wall thickness, shape and length. The tubes are designed with a diameter that is slightly larger than the diameter of the sperm head (5 μm). This fitting allows the sperm cells to be trapped inside the microtubes. The sperm cells provide a self-propulsion force to the microtubes, whereas the microtubes allow for steering based on their magnetic dipole. The resulting MBRs (Fig. 1) are autonomously controlled using an external magnetic field, as shown in Fig. 2.

2.2 Preparation of sperm-driven micro-bio-robots

The MBRs consist of ferromagnetic rolled-up microtubes that capture single bovine sperm cell. The sperm cell solution is prepared as follows: The previously cryopreserved bovine semen straws are removed from storage in liquid nitrogen and thawed for 10 minutes in the incubator at 37 °C. The thawed semen is diluted in 2 ml SP-TALP medium (modified Tyrode's Albumin Lactate Pyruvate Medium) and incubated for another 10 minutes at 37 °C. The coupling between motile sperm cells and microtubes is observed under the optical microscope after the addition of microtubes. We observe that the average swimming speed of the free cells decreases by 45 % after the coupling with the microtubes, as shown in Fig. 3.

3 Wireless magnetic-based control

An MBR consists of a rolled-up magnetic microtube that is coupled with a sperm cell. The microtube has an average length and diameter of 50 μm and 5-10 μm, respectively. Coupling between the magnetic tubes and the sperm cells happens randomly and allows the microtubes to overcome the viscous drag forces [11]. The magnetic torque (T(P)) exerted on the magnetic dipole of the microtubes is given by

$$\mathbf{T}(\mathbf{P}) = \mathbf{m} \times \mathbf{B}(\mathbf{P}), \tag{1}$$

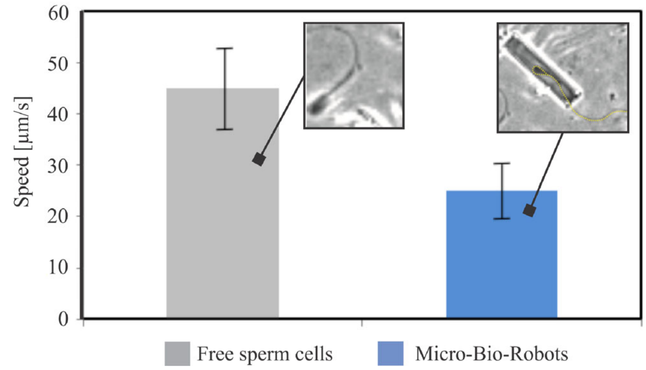

Fig. 3 Average speed of free sperm cells and the Micro-Bio-Robots. The speed of the free sperm cells [11] decreases by 45 % due to the coupling with the microtubes. Insets **a** and **b** show a free sperm cell and a coupled sperm cell with a microtube

where $\mathbf{m}$ and B(P) are the magnetic dipole moment of the MBR and the induced magnetic field at point (**P**), respectively. This magnetic torque allows the MBR to overcome the drag torque and align itself along the external magnetic field lines, as shown in Fig. 4. Reversing the uniform magnetic fields allow the MBR to perform *U-turn* trajectory. The drag torque is given by

$$\mathbf{T}_{\mathrm{d}}(\Omega) = \alpha\Omega, \tag{2}$$

where Ω is the angular velocity of the MBR. Further, α is the rotational drag coefficient and is given by

$$\alpha = \frac{\pi\eta l^3}{3}\left[\ln\left(\frac{l}{d}\right) + 0.92\left(\frac{d}{l}\right) - 0.662\right]^{-1}, \tag{3}$$

where l and d are the length and diameter of the MBR, respectively. In Eq. 3, η is the dynamic viscosity of the fluid ($\eta = 1.25$ mPa.s).

Our control strategy is based on directing the magnetic field lines towards a reference position using an orthogonal array of electromagnetic coils (Fig. 2). The propulsion force of the sperm cell allows the MBR to move along the field lines towards the reference position. The velocity of the MBR is not influenced by the magnetic field. This fact can be proven by the empty microtubes that are not propelled by a sperm flagellum, as shown in Fig. 5 by the red arrows. These tubes align to the external magnetic field, but do not move forward. This level of control is achieved using Eq. 1 by controlling the current at each of the electromagnets. The magnetic torque is mapped onto current using the following map

$$\mathrm{T}(\mathbf{P}) = \widehat{\mathbf{m}}\widetilde{\mathrm{B}}(\mathrm{P})\mathbf{I}. \tag{4}$$

In Eq. 4, $\mathbf{I}$ is the current vector and $\widehat{\mathbf{m}}\widetilde{\mathrm{B}}(\mathrm{P})$ is a constant matrix that maps current onto magnetic fields. This matrix depends on the magnetic dipole moment of the microtubes [23] and the configuration of the electromagnetic coils [19]. In Eq. 4, $\widehat{\cdot}$ is the cross-product operator [19]. We devise a proportional-derivative magnetic torque ($\mathrm{T}_{\mathbf{c}}(\mathrm{P})$) to orient the MBR along the field lines. This torque is given by [24]

$$\mathrm{T}_{\mathbf{c}}(\mathrm{P}) = \mathbf{K}_{\mathbf{p}}\mathbf{e} + \mathbf{K}_{\mathbf{d}}\dot{\mathbf{e}}, \tag{5}$$

where $\mathbf{K}_{\mathbf{p}}$ and $\mathbf{K}_{\mathbf{d}}$ are the proportional and derivative positive-definite gain matrices. Further, $\mathbf{e}$ and $\dot{\mathbf{e}}$ are the angular position tracking errors and its derivative, respectively. Setting the controlled torque (5) to (4), and solving for the current ($\mathbf{I}$) at each of the electromagnets allows us to orient the MBR towards a reference position based on the following error dynamics:

$$\dot{\mathbf{e}} + (\mathbf{K}_{\mathbf{d}} + \alpha\Pi)^{-1}\mathbf{K}_{\mathbf{p}}\mathbf{e} = 0. \tag{6}$$

In Eq. 6, $\alpha\Pi$ is the identity matrix. Further, $\mathbf{K}_{\mathbf{p}}$ and $\mathbf{K}_{\mathbf{d}}$ must be selected such that the matrix $((\mathbf{K}_{\mathbf{d}} + \alpha\Pi)^{-1}\mathbf{K}_{\mathbf{p}})$ is positive-definite.

The sperm-driven MBRs are contained inside a cubic glass vessel surrounded by the array of electromagnetic coils that provide the automated guidance of the MBRs.

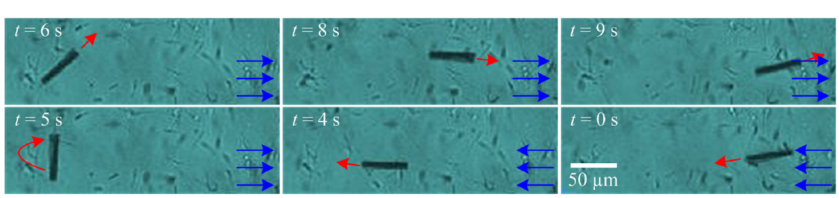

Fig. 4 The Micro-Bio-Robot (MBR) swims and undergoes a *U-turn* trajectory under the influence of uniform magnetic fields (*blue arrows*). The magnetic fields are reversed at time, $t = 5$ seconds. In this representative experiment, the MBR swims at a speed of 18 μm/s. The *U-turn* trajectory starts at time, $t = 0$ seconds (*bottom right image*)

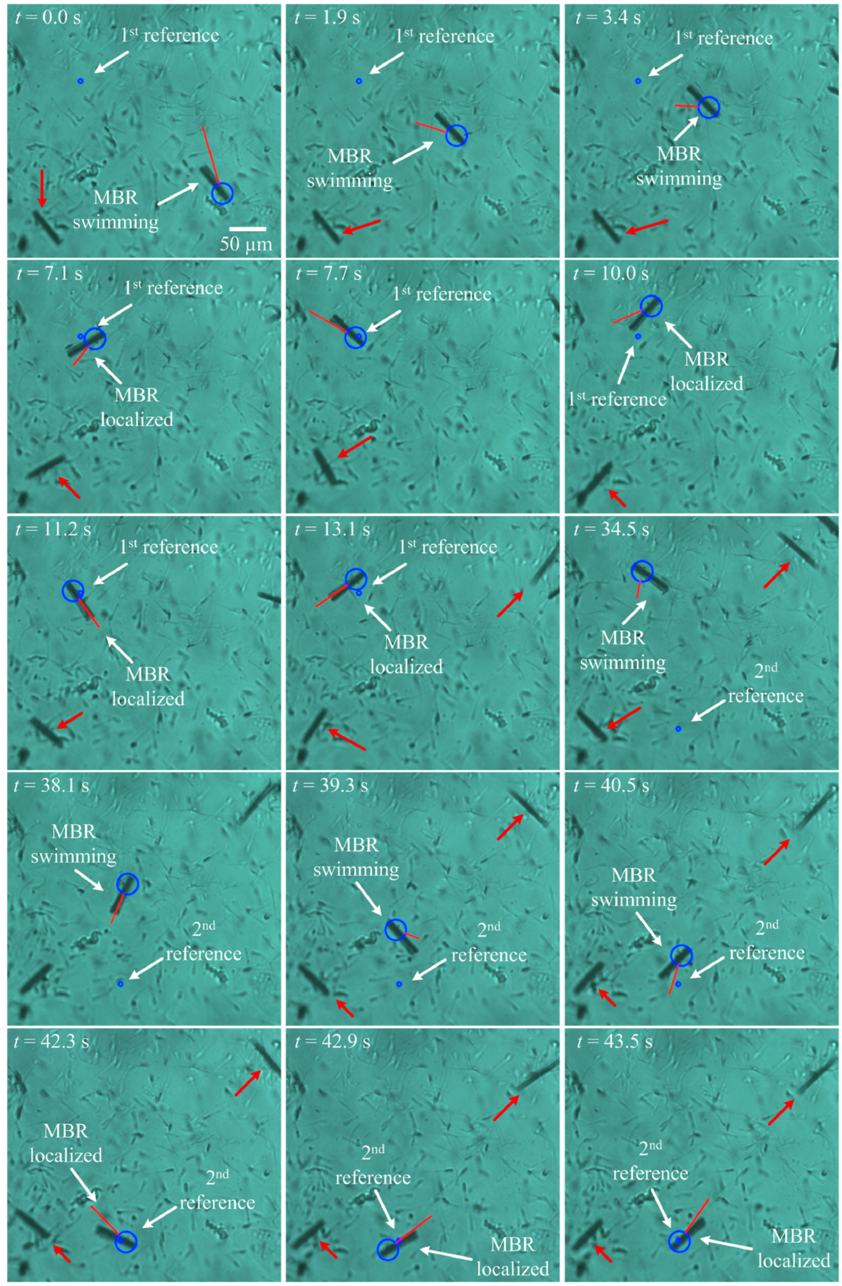

Fig. 5 A representative point-to-point closed-loop motion control of a Micro-Bio-Robot (MBR) towards 2 reference positions (*small blue circles*). The coupling between the sperm cells and some rolled-up microtubes allows them to swim. The *large blue circle* is assigned by our feature tracking algorithm [25] and the *red line* represent the velocity vector of the MBR. The *red arrows* indicate non-motile microtubes. Experiments are conducted at room temperature in modified Tyrode's Albumin-Lactate-Pyruvate Medium (SP-TALP). Please refer to the accompanying video that demonstrates the closed-loop motion control of the MBR

Motion of the MBR is tracked using a feature tracking algorithm and fed back to the closed-loop control system (5). Figure 5 shows a representative point-to-point motion control result of the MBR. Two reference positions are given to the control system at the time, $t = 0.0$ seconds and $t = 34.5$ seconds. We observed that the MBR moves towards the first reference position at an average speed of 33 μm/s, and is localized by the controlled magnetic fields within a circular region of 120 μm in diameter. At $t = 34.5$ seconds, the second reference position is given to the control system. The MBR moves towards this reference position at an average speed of 28 μm/s, and is localized within a circular region of 115 μm in diameter. In the left corner of the images in Fig. 5, a red arrow points out an empty microtube which acts as control object. This microtube aligns to the external magnetic field, but does not move out of its position.

The path of a controlled MBR is shown in Fig. 6. Five reference positions (vertical blue lines) are given to the control system to achieve point-to-point closed-loop control of the MBR. We observed that the MBR moves towards the reference positions at an average speed of 25 μm/s, and is localized within an average circular region of 90 μm in

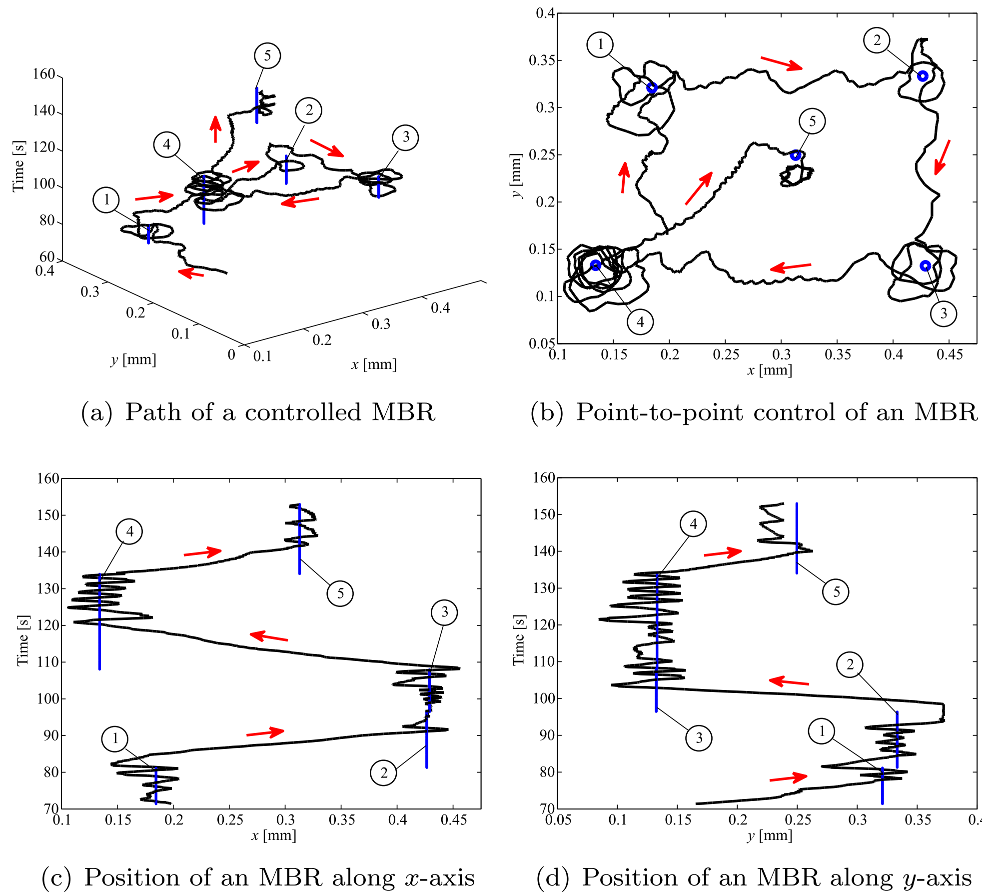

(a) Path of a controlled MBR

(b) Point-to-point control of an MBR

(c) Position of an MBR along x-axis

(d) Position of an MBR along y-axis

Fig. 6 Representative point-to-point motion control of a Micro-Bio-Robot (MBR) under the influence of the controlled magnetic fields. The *vertical lines* represent the reference positions. **a** The MBR moves towards 5 reference positions at an average speed of 25 μm/s. **b** The MBR is localized within an average region of 90 μm in diameter. **c** Path of the controlled MBR along x-axis. **d** Path of the controlled MBR along y-axis

diameter. Our control system can only localize the MBR within the reference position and cannot achieve zero position tracking error in the steady-state. This response is due to the continuous motion of the MBR as a result of the propulsion force of the sperm cell.

Furthermore, We determined the minimum magnetic field strength required for the alignment of the microtubes to be $\mathbf{B}(\mathbf{P}) = 1.39$ mT, which is much lower than previously estimated with permanent magnets [11]. However, magnetotactic bacteria and artificial bacterial flagella [5] require lower magnetic fields to algin along external magnetic field lines. This property is due to their lower rotational drag coefficients (rotational drag coefficient of the *M. magnetotacticum* strain MS-1 is 8.3×10^{-20} N.m.s), as opposed to that of the microtubes of the MBR (rotational drag coefficient of 7.5×10^{-17} N.m.s) [26]. Therefore, the magnetic field used to control the MBRs can be further decreased by increasing the thickness of the iron layers of the microtubes. Nevertheless, the accuracy provided by the proposed magnetic-based control and autonomous MBRs could allow them to be used in micro-manipulation, micro-assembly, micro-actuation, and applications that are not yet conceived.

Additionally, we demonstrate that the sperm-driven MBR is guided to a 100 μm magnetic microparticle. As shown in Fig. 7, the electromagnetic coil setup can be used to steer the MBR to a desired object (magnetic microparticle). When the sperm flagella-driven MBR reaches the magnetic microbead, it attaches to it due to the magnetic attraction. This experiment demonstrates the application of this closed-loop magnetic control setup for guiding purposes of MBR.

4 Discussion

It is essential to decrease the size of the sperm-driven MBRs to enable access to deep-seated regions in the human body. Our MBRs have an average diameter of 5-8 μm, whereas the smallest capillaries of the human blood circulatory system have diameters which range from 6 to 10 μm [18]. Therefore, it is important to decrease the size of the MBRs to make them viable for targeted drug delivery and other biomedical applications [10]. The MBR based on bull spermatozoa captured inside microtubes can be modified and applied to spermatozoa of any other species. This technology is also tested using mouse spermatozoa, and coupling with the microtubes is observed as reported in this study. Therefore, it is possible to scale the size of the MBRs depending on the size of spermatozoa that ranges from

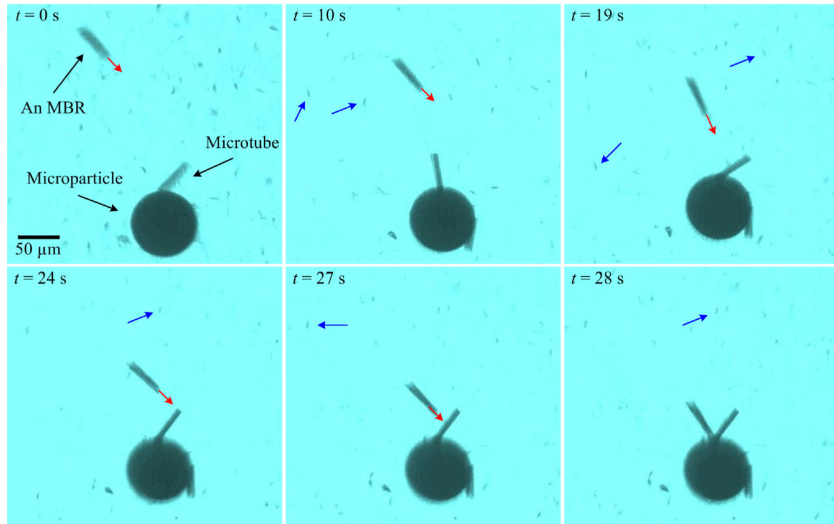

Fig. 7 The Micro-Bio-Robot (MBR) targets a microparticle with a diameter of 100 μm. The MBR swims at an average speed of 5 μm/s. This representative motion control experiment shows that the MBR can be used to selectively target a microobject under the influence of its self-propulsion force and controlled magnetic fields. The *blue arrows* indicate living sperm cells that are not attached to the microtubes

1.4 μm head width in wallabies to 17.5 μm head width in Asiatic musk shrews [27]. In addition to the application in drug delivery, in the light of harnessing this technology for the development of new assisted reproduction technologies, one vision for the sperm-driven MBRs is the capture and delivery of human spermatozoa to the oocyte *in-vivo*.

5 Conclusions and future work

We demonstrate the closed-loop point-to-point motion control of an MBR under the influence of the controlled magnetic fields. The magnetic dipole moment of the rolled-up microtubes and the propulsion force provided by the sperm cells allows the MBR to move at an average speed of 25 μm/s. This control system using electromagnetic coils and feature tracking algorithm allows for more reproducible motion control of sperm-driven microtubes with a fairly low magnetic field strength of 1.39 mT. Further, the control system allows for the localization of the MBRs within a circular region of 90 μm in average diameter. The demonstration of the two-dimensional magnetic remote control of the sperm-driven microtube is an important step towards the application of this kind of MBRs in the biomedical field that achieves the controlled guidance of a single sperm cell in physiological environments.

As part of future studies, the efficiency of MBRs will be increased by decreasing the length of the microtubes. This decrease would allow the sperm tail to have larger beating amplitudes, as opposed to that achieved using our current microtubes. In addition, characterization and control of the MBRs in three-dimensional space will be done. Furthermore, the effect of time-varying flow rates on the motion of the MBRs inside microfluidic channels will be studied.

Acknowledgments The authors acknowledge the funding from MIRA-Institute for Biomedical Technology and Technical Medicine, University of Twente. The research leading to these results has also received funding from the Volkswagen Foundation (# 86 362) and the European Research Council under the European Unions Seventh Framework Programme (FP7/2007-2013)/ERC Grant agreement No. 311529.

References

1. Purcell EM (1977) Am J Phys 45(1):3–11
2. Mallouk TE, Sen A (2009) Sci Am 300:72–77
3. Loget G, Kuhn A (2011) Nat Commun 2(535):1–6
4. Ghosh A, Fischer P (2009) Nano Lett 9(6):2243–2245
5. Peyer KE, Zhang L, Nelson BJ (2013) Nanoscale 5(4):1259–1272
6. Dreyfus R, Baudry J, Roper ML, Fermigier M, Stone HA, Bibette J (2005) Nature 436(6):862–865
7. Zhang L, Petit T, Peyer KE, Nelson BJ (2012) Nanomed: Nanotechnol. Biol Med 8(7):1074–1080
8. Bell DJ, Leutenegger S, Hammar KM, Dong LX, Nelson BJ (2007) In: Proceedings of the IEEE international conference in robotics and automation (ICRA). pp 1128–1133
9. Tottori S, Zhang L, Qiu F, Krawczyk K, Franco-Obregn A, Nelson BJ (2012) Adv Mater 24(6):811–816
10. Wang J, Gao W (2012) ACS Nano 6(7):5745–5751
11. Magdanz V, Sanchez S, Schmidt OG (2013) Adv Mater 25(45):6581–6588
12. Martel S, Felfoul O, Mathieu J-B, Chanu A, Tamaz S, Mohammadi M, Mankiewicz M, Tabatabaei N (2009) Int J Robot Res 28(9):1169–1182
13. Khalil ISM, Pichel MP, Abelmann L, Misra S (2013) Int J Robot Res 32(6):637–649
14. Pan Y, Du X, Zhao F, Xu B (2012) Chem Soc Rev 41:2912–2942
15. Khlebtsov N, Dykman L (2011) Chem Soc Rev 40(3):1647–1671
16. Mei YF, Huang G, Solovev AA, Urena EB, Munch I, Ding F, Reindl T, Fu RKY, Chu PK, Schmidt OG (2008) Adv Mater 20(21):4085–4090

17. Bermudez Urena E, Mei YF, Coric E, Makarov D, Albrecht M, Schmidt OG (2009) Phys D: Appl Phys 42(5)
18. Nelson BJ, Kaliakatsos IK, Abbott JJ (2010) Ann Rev Biomed Eng 12:55–85
19. Kummer MP, Abbott JJ, Kartochvil BE, Borer R, Sengul A, Nelson BJ (2010) IEEE Trans Robot 26(6):1006–1017
20. Xi W, Solovev AA, Ananth A, Gracias D, Sanchez S, Schmidt OG (2013) Nanoscale 5:1294–1297
21. Kagan D, Benchimal MJ, Claussen JC, Chuluun-Erdene E, Esener S, Wang J (2012) Angew Chem Int Ed 51:7519–7522
22. Solovev AA, Xi W, Gracias D, Harazim SM, Deneke C, Sanchez S, Schmidt OG (2012) ACS Nano 6:1751
23. Khalil ISM, Magdanz V, Sanchez S, Schmidt OG, Misra S (2013) IEEE Trans Robot 30. doi:10.1109/TRO.2013.2281557
24. Khalil ISM, Magdanz V, Sanchez S, Schmidt OG, Misra S (2013) Appl Phys Lett 103:172404
25. Keuning JD, de Vries J, Abelmann L, Misra S (2011) In: Proceedings of the IEEE international conference of robotics and systems (IROS). pp 421–426
26. Khalil ISM, Magdanz V, Sanchez S, Schmidt OG, Misra S (2013) In: Proceedings of the IEEE international conference of robotics and systems (IROS). pp 2035–2040
27. Cummins JM, Woodall PF (1985) J Reprod Fert 75:153–175